High order sliding mode direct torque control of a DFIG supplied by a five-level SVPWM inverter for the wind turbine

Ahmed Bourouina [1], Abdelkader Djahbar [2], Abdelkader Chaker [1], Zinelaabidine Boudjema[2]

[1] Electrical Engineering Department ENP Oran, Algeria
[2] Hassiba Benbouali University, B.P 78C , Ouled Fares Chlef, 02180, Algeria
E-mail: ahmed_bourouina@yahoo.fr

Abstract. The paper presents a new direct-torque control (DTC) strategy based on a second-order sliding mode of a doubly-fed induction generator (DFIG) integrated in a wind turbine system (WTS). In the first step we propose to use a five-level inverter based on the space-vector pulse-width modulation (SVPWM) to supply the DFIG rotor side. This is the harmonic distortion of the DFIG rotor voltage and then performs provides the power to the grid by the stator side. The conventional DTC (C-DTC) using hysteresis controllers has considerable flux and torque ripples at a steady-state operation. In order to ensure a robust DFIG DTC strategy and reduce the flux and torque ripples, a second-order sliding-mode method is used in the second step. The Simulation results show the efficiency of the proposed control method especially in terms of the quality of the provided power compared to C-DTC.

Keywords: DFIG, wind turbine, five-level SVPWM inverter, DTC, sliding mode.

Neposredno krmiljenje navora v drsnem načinu drugega reda pri dvojno napajanem asinhronskem generatorju v vetrnih elektrarnah

V prispevku smo predstavili neposredno krmiljenje navora v drsnem načinu drugega reda pri dvojno napajanem asinhronskem generatorju v vetrnih elektrarnah. V prvem koraku smo predlagali uporabo petstopenjskega pretvornika, ki temelji na prostorski vektorski pulznоширinski modulaciji. S tem zmanjšamo vpliv višjeharmonskih komponent. Zmanjšanje magnetnega pretoka in nihanje navora smo dosegli z uporabo drsnega načina drugega reda. Rezultati simulacij potrjujejo učinkovitost predlaganega krmiljenja, še zlasti kakovost električne energije v primerjavi s klasičnim načinom krmiljenja.

1 INTRODUCTION

In the recent years, wind-energy technology has drawn much attention of research groups and industry. This has been confirmed by a large number of research papers published over this period of time. Nowadays, the variable-speed WTS based on DFIG is the most used system in onshore wind farms [1]. The major DFIG advantage is that the rotor-side converter is sized for only 30% of rated power compared to other generators used in the variable-speed WTSs. So, the cost of the converter is lowered [2].

In a usual DFIG-based WTS, the generator rotor side is generally fed by a two-level inverter. Due to its advantages, which include a minimized (dv/dt) stress, lower harmonics and lesser common-mode voltages, the multi-level inverters has found several applications in the domain of high-power medium-voltage systems [3] such as electric vehicles, traction drives [4], static variable compensators [5], and more recently, wind power systems [6]. These features have made it suitable for application in large and medium induction-machine drives. In this work, a five-level SVPWM inverter is used in the DFIG drive.

The stator-field-oriented control using proportional-integral (PI) controllers is conventional control scheme used for the DFIG-based WTS [7, 8]. In this control scheme, decoupling between the d and q axis current is achieved with a feed-forward compensation making the DFIG model less complex and making the use of PI controllers. However, this control strongly depends on the machine parameters, it uses multiple loops and requires much control effort to guarantee the structure stability over the total speed range [9].

To overcome the disadvantages of the vector control, DTC is used [10]. In C-DTC, the torque and flux can be directly controlled by using a switching table and hysteresis controllers. Nevertheless, there are a few difficulties that limit the use of these controllers, such as a variable switching frequency and torque ripple [11]. In many research papers, these adverse effects are reduced by using a space-vector modulation (SVM) technique, however the robustness of the control is immolated [12, 13].

Recently, the sliding-mode control (SMC) methodology has been widely used for a robust control of nonlinear systems. SMC based on the theory of

variable-structure systems has attracted a lot of research on control systems. In the last two decades [14]. A robust control is achieved by adding a discontinuous control signal across the sliding surface to satisfy the sliding condition. However, the deficiency of this type of control is the chattering phenomenon caused by a discontinuous control action. To resolve this problem, several modifications to the usual control law have been proposed. In most cases, the boundary-layer approach is applied [15].

Some useful solutions for the sliding mode DTC with lower torque and flux ripples used in the induction-motor drive are described in [10, 16]. In [16], the authors propose to use DTC with a super twisting SMC applied to the induction-motor drive.

In a robust DTC without torque and flux ripples and with a lower chattering phenomenon, the paper we proposes to use a second-order sliding-mode direct-torque control (SOSM-DTC) for the DFIG drive integrated in WTS. This contol reduces the mechanical stress and improves the power quality provided to the grid. The newly developed second-order sliding-mode generalizes the basic sliding-mode scheme that acts on the second-order time derivatives of the structure variation since the constraint instead of influencing the initial variation derivative as it occurs in usual sliding modes [17]. Some of such controllers were reported in the literature [18-21].

The paper is organizred as follows. The DFIG model is presented in Section 2. Modeling and control of a five-level SVPWM are discussed in Section 3. In Section 4 DFIG SOSM-DTC scheme is applied. The effectiveness of the proposed strategy is demonstrated by simulation results given in Section 5.

2   MODEL DFIG

In literature, the DFIG Park model is widely used [22]. The equations voltage and flux for the DFIG stator and rotor in the Park reference frame are given by:

$$
\begin{cases}
V_{ds} = R_s I_{ds} + \dfrac{d}{dt}\psi_{ds} - \omega_s\psi_{qs} \\[4pt]
V_{qs} = R_s I_{qs} + \dfrac{d}{dt}\psi_{qs} + \omega_s\psi_{ds} \\[4pt]
V_{dr} = R_r I_{dr} + \dfrac{d}{dt}\psi_{dr} - \omega_r\psi_{qr} \\[4pt]
V_{qr} = R_r I_{qr} + \dfrac{d}{dt}\psi_{qr} + \omega_r\psi_{dr}
\end{cases}
,\quad
\begin{cases}
\psi_{ds} = L_s I_{ds} + M I_{dr} \\
\psi_{qs} = L_s I_{qs} + M I_{qr} \\
\psi_{dr} = L_r I_{dr} + M I_{ds} \\
\psi_{qr} = L_r I_{qr} + M I_{qs}
\end{cases}
\tag{1}
$$

where (V_{ds}, V_{qs}, V_{dr}, V_{qr}), (I_{ds}, I_{qs}, I_{dr}, I_{qr}), (ψ_{ds}, ψ_{qs}, ψ_{dr}, ψ_{qr}) are the stator and rotor voltages, currents and fluxes, respectively R_s and R_r are the resistances of the rotor and stator windings, respectively L_s, L_r and M are the inductance own stator, rotor, and the mutual inductance between the two coils respectively.

The stator and rotor pulsations and the rotor speed are interconnected by the following equation:

$$\omega_s = \omega + \omega_r.$$

where ω_s and ω_r are the stator and rotor electrical pulsations respectively, and ω is the mechanical one.

The DFIG mechanical equation is:

$$
C_{em} = C_r + J \cdot \frac{d\Omega}{dt} + F_r \cdot \Omega \tag{2}
$$

where we the electromagnetic torque C_{em} can be expressed as follows:

$$
C_{em} = \frac{3}{2} n_p \frac{M}{L_s}(\psi_{qs} I_{dr} - \psi_{ds} I_{qr}) \tag{3}
$$

where C_r is the load torque, Ω is the mechanical rotor speed, J is the inertia, F_r is the viscous friction coefficient and n_p is the number of pole pairs.

The active and reactive powers of the stator side are defined as :

$$
\begin{cases}
P_s = \dfrac{3}{2}(V_{ds} I_{ds} + V_{qs} I_{qs}) \\[6pt]
Q_s = \dfrac{3}{2}(V_{qs} I_{ds} - V_{ds} I_{qs})
\end{cases}
\tag{4}
$$

To develop a decoupled control of the stator active and reactive power, the Park reference frame linked to the stator flux is used (Figure 1).

Assuming that the is d-axis oriented along the stator flux position following equation (1) and disregarding R_s, we can write :

$$
\psi_{ds} = \psi_s \quad \text{and} \quad \psi_{qs} = 0 \tag{5}
$$

$$
\begin{cases}
V_{ds} = 0 \\
V_{qs} = \omega_s \psi_s
\end{cases}
\tag{6}
$$

$$
\begin{cases}
I_{ds} = -\dfrac{M}{L_s} I_{dr} + \dfrac{\psi_s}{L_s} \\[6pt]
I_{qs} = -\dfrac{M}{L_s} I_{qr}
\end{cases}
\tag{7}
$$

By using equations (6) and (**7**), equation (4) can be written as follows :

$$
\begin{cases}
P_s = -\dfrac{3}{2}\dfrac{\omega_s \psi_s M}{L_s} I_{qr} \\[8pt]
Q_s = -\dfrac{3}{2}\left(\dfrac{\omega_s \psi_s M}{L_s} I_{dr} - \dfrac{\omega_s \psi_s{}^2}{L_s}\right)
\end{cases}
\tag{8}
$$

The electromagnetic torque can then be expressed by:

$$
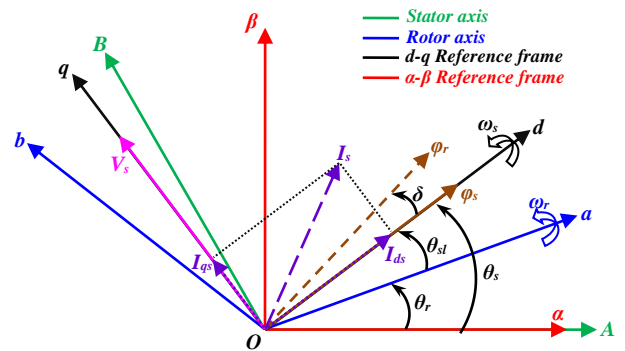C_{em} = -\frac{3}{2} n_p \frac{M}{L_s} I_{qr} \psi_{ds} \tag{9}
$$

Figure 1. Field-oriented control technique.

3 FIVE-LEVEL SOURCE-VOLTAGE-INVERTER MODELING

3.1. CONFIGURATION OF A FIVE-LEVEL CONVERTER

The principal circuit structure of a three-phase source vector inverter is shown in Figure 2. Each of the converter phases is composed of eight IGBT switches with six clamp diodes. The higher number of levels increases the power rating and lower the output harmonics [23].

For each device in Figure 2, the On/Off sequence should take into account two imperatives; three of the switches should be constantly "on" and the other three constantly "off". For a similar leg, the superior and inferior switches are controlled with two reverse pulseing signals. Consequently, no perpendicular conduction is feasible and care should be taken that there is no interruption in the power switch transition. As shown in Table, for each phase leg, the five-level inverter has 125 switching combinations, eight switching devices, six clamping diodes and four DC-side capacitors. It generates a five-level phase voltage, nine-level line voltage waves, 5^3-$(5-1)^3$ voltage space vectors and $6^{(5-1)}$ number of the triangle (Figure 3) [23].

3.2 SVPWM technique

The SVPWM technique refers to a particular switching cycle of the higher three switches of a six-phase power inverter. This technique is applied to produce less harmonic distortions in the DFIG rotor-side voltages and guarantees a more efficient use of the supply voltage unlike is the case with the conventional sinusoidal modulation technique.

The SVPWM technique is used to estimate the popular reference-voltage vector for the eight switching designs. Eq. (10) demonstrates that for each PWM period, the voltage can be estimated by having the power inverter in switching model V_x, $V_{x\pm60}$ and zero-vector $O(000)$ or (111) T_1, T_2 and T_0 for the time interval.

$$T_{PWM}.V = T_1.V_x + T_2.V_{x\pm60} + T_0(O_{000} \text{ or } O_{111}) \qquad (10)$$

where $T_1 + T_2 + T_3 = T_{PWM}$.

As shown in Figure 3, in the cover of the hexagonal shaped by the diverse switching locations of the five-level inverter, the angle between the two neighboring non-zero vectors is 60°, The zero vectors are at the starting point and by affect the DFIG zero voltage [23]. The hexagonal is the location of maximum v Thus, the v magnitude should be restricted to a smaller radius of this cover when v is a turning vector. This gives the maximum magnitude of $V_{dc}/\sqrt{2}$ for v. Likewise, as seen in Figure 3, the greatest rms values of the basic line-to-line and line to neutral output voltage are $V_{dc}/\sqrt{2}$ and $V_{dc}/\sqrt{2}$, which is $2/\sqrt{3}$ times more than the sinusoidal PWM strategy can produce.

If should be note of that the obtained waveforms are a time-averaged edition of the PWM switching signals they apparently illustrate the fundamental frequency at ω_s and the third harmonic at $3\omega_s$ which is intrinsically caused by the space-vector approach.
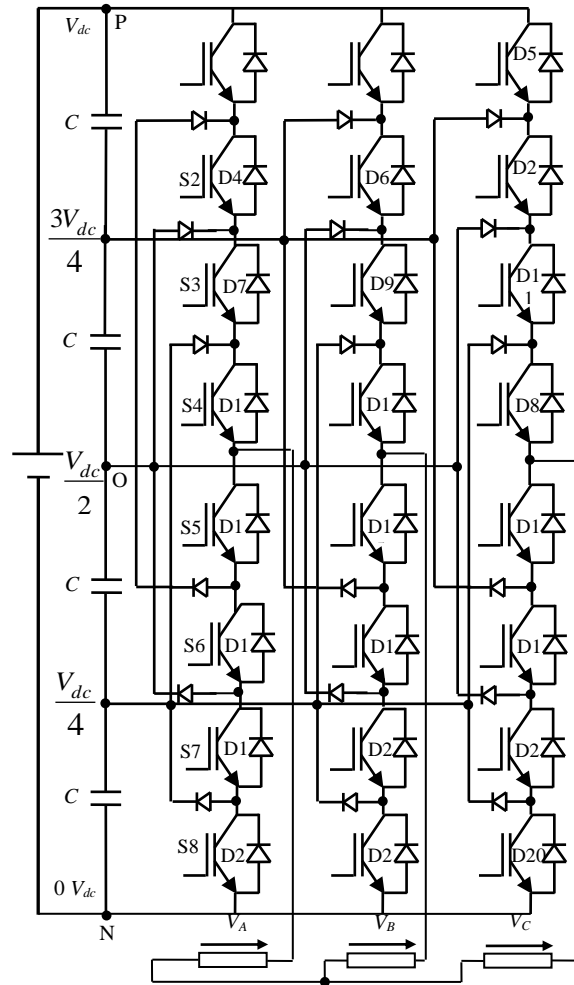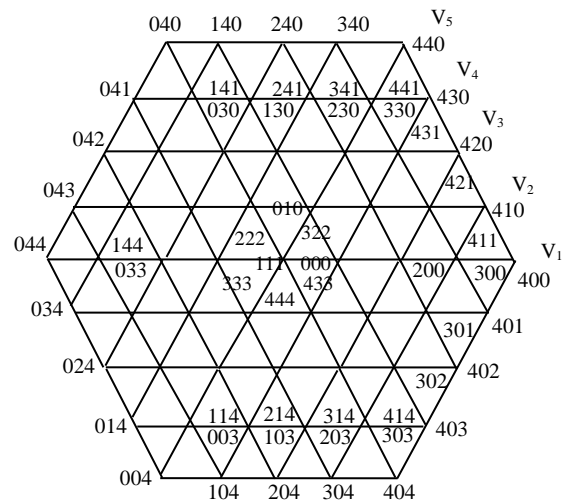

Figure 2. Five-level circuit configuration.

Figure 3. Space vector locations for the five-level inverter.

4 SECOND-ORDER SLIDING-MODE DIRECT-TORQUE CONTROL (SOSM-DTC) OF DFIG

The SOSM-DTC technique is used to control the DFIG torque and rotor-flux magnitude. The flux is controlled by direct-axis voltage (V_{dr}), and the torque is controlled by quadrature-axis voltage (V_{qr}).

The chattering phenomenon which represents a big problem for the conventional SMC can be very hazardous for DFIG because an interrupted control can overheat of the coils and excite some undesirable high-frequency dynamics [23]. Some solutions to avoid this drawback are in[14, 24].

The major idea is to adjust the dynamics in small region of the discontinuity surface to evade a real discontinuity and at the same time to conserve the major characteristics of the whole system. The proposed, high-order sliding-mode (HOSM) generalizes the basic sliding-mode idea that affects on the high-order time derivatives of the system deviation from the constraint instead of affecting the first deviation derivative as it happens in standard sliding modes [25-27]. Besides advantages the major privileges of the original technique, the chattering effect and need of higher accuracy are discussed in a practical implementation. in the last two decades these controllers have been subject of many research papers [18, 19].

The major difficulty in the HOSM algorithm implementation is the increasing need for information. In fact, the knowledge of $\dot{S}, \ddot{S}, ..., S^{(n-1)}$ is necessary for the designing an nth-order controller. Among all the algorithms proposed for HOSM, the super-twisting algorithm is an exception, as it requires only the information about the sliding surface [20]. Consequently, this algorithm is used for the proposed control strategy. As shown in [21], using this algorithm assures stability of any SOSM controller.

The proposed SOSM-DTC is designed to control the DFIG rotor flux and electromagnetic torque shown in Figure 4.

The SOSM controller of the rotor flux and torque is used to affect the two rotor voltage components as in Eqs. (11) and (12) [16,28].

$$V_{dr} = K_1 |S_{\varphi r}|^r \text{sign}(S_{\varphi r}) + V_{dr1} \tag{11}$$
$$\dot{V}_{dr1} = K_2 \text{sign}(S_{\varphi r})$$

$$V_{qr} = K_1 |S_{Cem}|^r \text{sign}(S_{Cem}) + V_{qr1} \tag{12}$$
$$\dot{V}_{qr1} = K_2 \text{sign}(S_{Cem})$$

where the sliding-mode variables are the flux ($S_{\varphi r} = \varphi_r^* - \varphi_r$)and the torque error ($S_{Cem} = C_{em}^* - C_{em}$) and the control gains (K_1 and K_2) check the stability condition.

4.1. STABILITY AND GAIN CHOICE

Let us consider a dynamic system with input u, state x and output y given by :

$$\frac{dx}{dt} = a(x,t) + b(x,t)u, \quad y = c(x,t) \tag{13}$$

It is difficult to determine the input function
($u = f(y, \dot{y})$) which drives the system trajectories toward the starting point of the phase plane in a limited period of time. The input (u) is a novel state variable, whereas the switching control is appended to its time derivative ($\dot{u}$). The output (y) is controlled by an SOSM controller.

$$u = K_1 |S|^r \text{sign}(S) + u_1 \tag{14}$$
$$\dot{u}_1 = K_2 \text{sign}(S)$$

Where the sliding variable is $S = y^* - y$.

The controller does not use the derivative of the sliding variable. As in Eq. (14), an adequate condition is required for convergence to the sliding surface and for the gain stability [16]:

$$K_1 > \frac{A_M}{B_m}, \quad K_2 \geq \frac{4A_M}{B_m^2} \cdot \frac{B_M(K_1 + A_M)}{B_m(K_1 - A_M)} \tag{15}$$

Where $A_M \geq |A|$ and $B_M \geq B \geq B_m$ are upper and lower limit of A and B in the second derivative of y.

$$\frac{d^2 y}{dt^2} = A(x,t) + B(x,t)\frac{du}{dt} \tag{16}$$

5 SIMULATION RESULTS

simulations are carried out with a 1.5 MW DFIG attached to a 398V/50Hz grid and supplied through the rotor side of a five-level SVPWM inverter by using the Matlab/Simulink environment. The machine parameters are: $n_p = 2$, $R_s = 0.012$ Ω, $R_r = 0.021$ Ω, $L_s = 0.0137$ H, $L_r = 0.0136$ H, $M = 0.0135$ H, $F_r = 0.0024$ Nm/s, $J = 1000$ kg.m^2 and $R = 35.25$ m.

The DTC and SOSM-DTC control strategies are simulated and compared in terms of reference tracking, stator-current harmonic distortion and robustness against the machine-parameter variations.

5.1. REFERENCE TRACKING TEST

The objective of this test is to study the behaviour of the two DTC control strategies while the DFIG speed is kept at its nominal value. Figures 5-8 show the obtained simulation results. As seen from Figures 5 and 6, the torque and rotor flux almost perfectly track their reference values. Contrary to the C-DTC strategy where the coupling effect between the two axes is apparent, the SOSM-DTC decouples them. On the other hand, Figures 7 and 8 show the harmonic spectra of one DFIG phase-stator current obtained using the Fast Fourier Transform (FFT) technique for each control strategy. As well seen from Figure 7, for SOSM-DTC (THD = 1.31%) the total harmonic distortion (THD) is reduced compared to C-DTC (THD = 2.22%) with a two-level inverter and THD

is further reduced when using the five-level SVPWM inverter (THD = 0.85%) (Figure 8). on following the above, SOSM-DTC is more competitive than C-DTC for the DFIG-based WTS applications, especially when using a five-level SVPWM inverter.

5.2. ROBUSTNESS TEST

To analyze robustness of the employed DTC control strategies, the machine are changed. The values of the stator and rotor resistances (R_s and R_r) are doubled and the values of the inductances (L_s, L_r and M) are divided by 2. The machine runs at its nominal speed. As seen from the simulation results given in Figure 9. The DFIG parameter variations increase slightly the time response of the C-DTC strategy. On the other hand these variations affect the torque and flux curves, this effect is more important for C-DTC than the SOSM-DTC effect. Thus, the conclusion to be drawn is that the SOSM-DTC strategy is more robust than the C-DTC one.

6 CONCLUSION

The paper presentes a SOSM-DTC scheme of a DFIG connected directly to the grid by the stator side and fed by a five-level SVPWM inverter from the rotor side.

First, a DFIG model is made .To provide power to the grid by the DFIG stator side, a five-level SVPWM power inverter is used. SOSM-DTC is synthesized and compared to C-DTC. In ideal condition (no parameters variations and no disturbances), both DTC strategies track almost perfectly their references except that a coupling effect appeares in the C-DTC responses and there is none in the SOSM-DTC ones. The simulation results show that SOSM-DTC operates with a much lower chattering phenomenon. Using a five-level SVPWM inverter minimizes the power harmonic distortion. A robustness test is made after modifying the DFIG parameters, the modification induces some disturbances in the torque and flux responses, with an almost double effect when using the C-DTC strategy. The conclusion drawn from these results is that SOSM-DTC equipped with a five-level SVPWM inverter provides a robust control and can be considered a very attractive solution for the devices using DFIG, such as the wind-energy conversion systems.
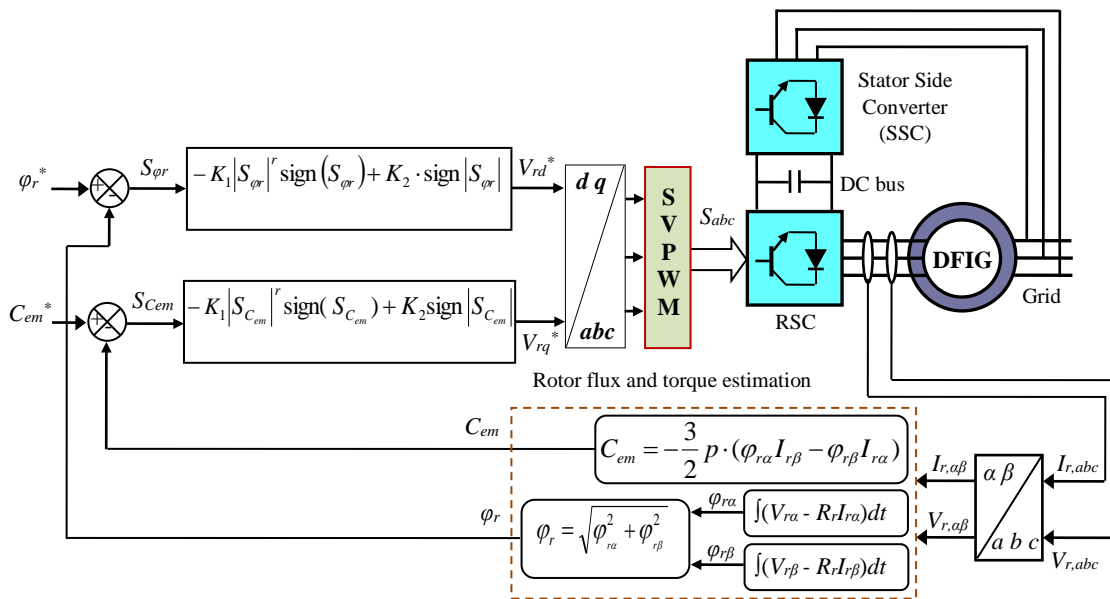

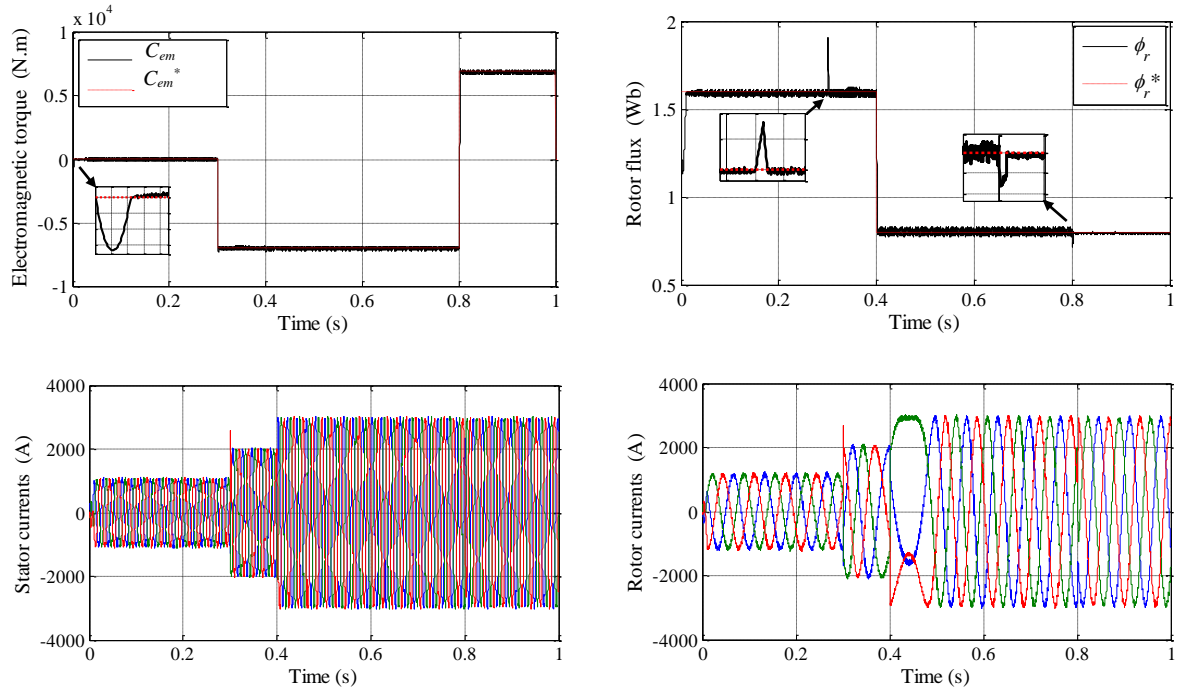Figure 4 . Bloc diagram of DFIG with SOSM-DTC.

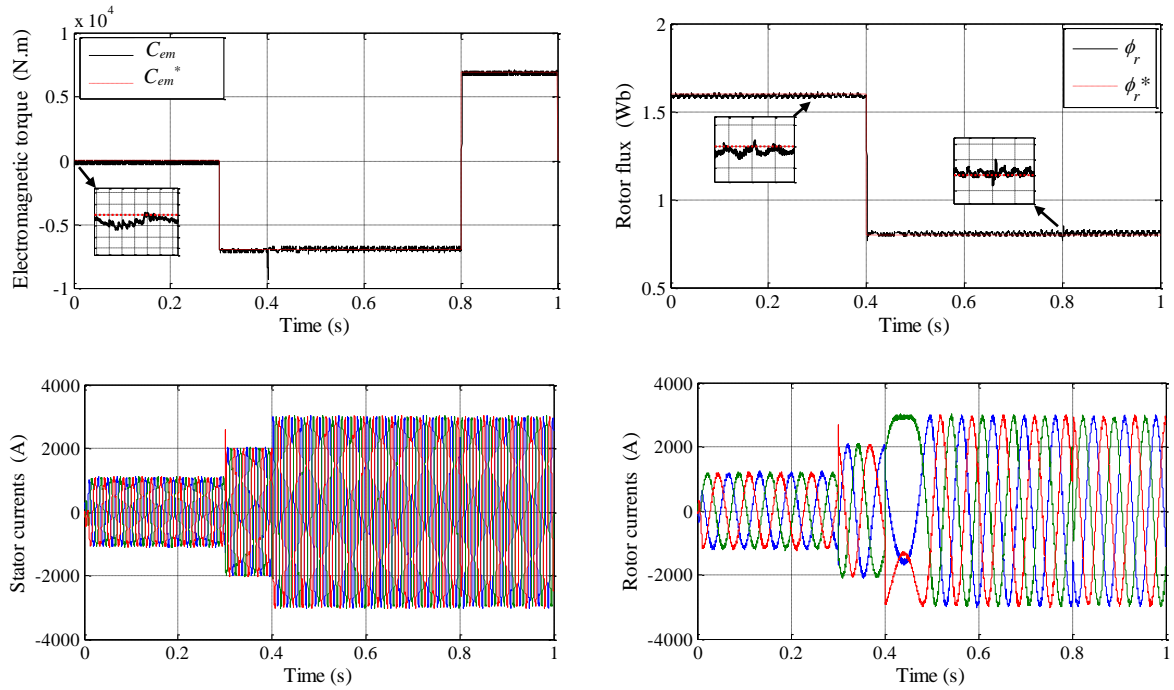Figure 5. C-DTC strategy responses (reference tracking test).

Figure 6. SOSM-DTC strategy responses (reference tracking test).
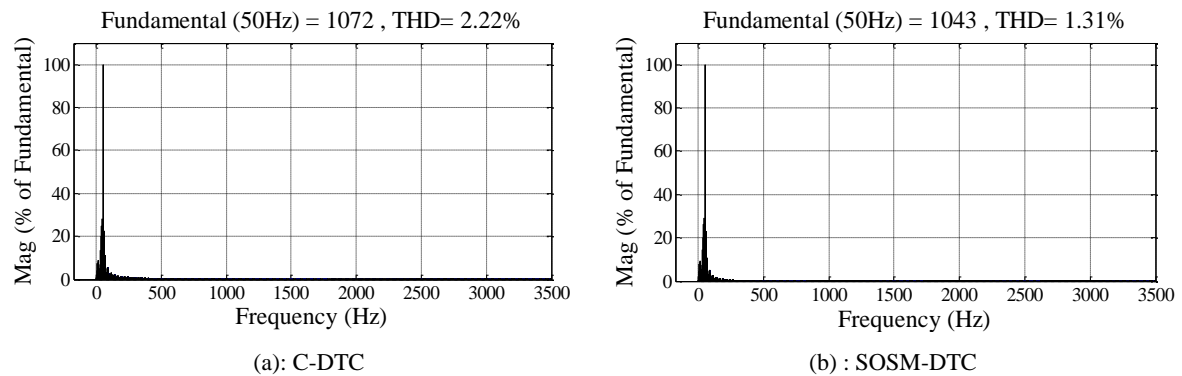
(a): C-DTC

(b) : SOSM-DTC

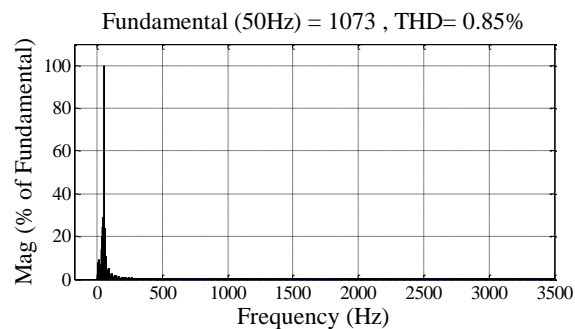Figure 7. THD of a one-phase stator current for DFIG supplied by a two-level inverter.

Figure 8. THD of a one-phase stator current for a DFIG supplied by a five-level SVPWM inverter.
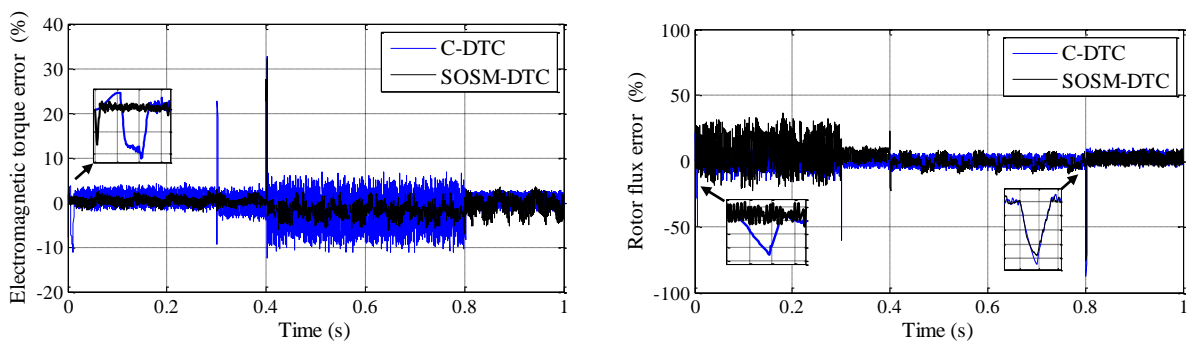

Figure 9. Error curves (robustness test).

REFERENCES

[1]   A. Kerboua., M. Abid. Hybrid fuzzy sliding mode control of doubly-fed induction generator speed in wind turbines. Journal. of Power Technologies, Vol. 95, No. 2, 2015, pp. 126–133.

[2]   S. Massoum, A. Meroufel, A. Massoum, P. Wira. A direct power control of the doubly-fed induction generator based on the SVM Strategy. Elektrotehniški vestnik, Vol. 84, No. 5, 2017, pp. 235-240.

[3]   T. Karaipoom, I. Ngamroo. Optimal superconducting coil integrated into DFIG wind turbine for fault ride through capability enhancement and output power fluctuation suppression. IEEE T Sustain Energ, Vol. 6, 2014, pp. 28–42.

[4]   K. K. Gupta, S. Jain. Comprehensive review of a recently proposed multilevel inverter. IET Power Electron., Vol. 7, No. 3, 2014, pp. 467–479.

[5]   A. Kolli, O. Béthoux, A. De Bernardinis, E. Labouré, G. Coquery. Space-vector PWM control synthesis for an H-bridge drive in electric vehicles. IEEE Trans. Veh. Technol., Vol. 62, No. 6, 2013, pp. 2441–2452.

[6]   J.A. Barrena, L. Marroyo, M.A.R. Vidal, J.R.T. Apraiz. Individual voltage balancing strategy for PWM cascaded H-bridge converter based STATCOM. IEEE Trans. Ind. Electron., Vol. 55, No. 1, 2008, pp. 21–29.

[7]   P. Samuel, R. Gupta, D. Chandra. Grid interface of wind power with large split-winding alternator using cascaded multilevel inverter. IEEE Trans. Energy Convers., Vol. 26, No. 1, 2011, pp. 299-309.

[8]   A.M. Rao, N.K. Kumar, K. Sivakumar. A multi-level inverter configuration for 4n pole induction motor drive by using conventional two-level inverters. In: IEEE 2015

International Conference on Industry Technology, 17-19 March 2015; Seville, Spain: IEEE. pp. 592-597.

[9] Y. Zhang, Z. Li, T. Wangy, W. Xuy, J. Zhuy. Evaluation of a class of improved DTC method applied in DFIG for wind energy applications. IEEE 2011 International Conference on Electrical Machines and Systems, 20-23 August 2011; Beijing, China: IEEE. pp. 2037-2042.

[10] S.E. Ardjoun, M. Abid. Fuzzy sliding mode control applied to a doubly fed induction generator for wind turbines. Turk J Elec Eng & Comp Sci, Vol. 23, 2015, pp. 1673-1686

[11] J. Sayritupac, E. Albánez, J. Rengifo, J.M. Aller and J. Restrepo. Predictive Control Strategy for DFIG Wind Turbines with Maximum Power Point Tracking Using Multilevel Converters. IEEE Workshop on *Power Electronics and Power Quality Applications (PEPQA)*, 2-4 June 2015, Bogota, pp. 1-6.

[12] G.S. Buja, M.P. Kazmierkowski Direct torque control of PWM inverter-fed AC motors - a survey. IEEE T Ind Electron, Vol. 51, 2004, pp. 744-757.

[13] S.Z. Chen, N.C. Cheung, K.C. Wong, J. Wu .Integral sliding-mode direct torque control of doubly-fed induction generators under unbalanced grid voltage. IEEE T Energy Conver, Vol. 25, 2010, pp. 356-368.

[14] X. Zhu, S. Liu, Y. Wang. Second-order sliding-mode control of DFIG-based wind turbines. In: IEEE 2014 3rd Renewable Power Generation Conference, 24-25 September 2014; Naples, Italy: IEEE. pp. 1-6.

[15] K.D.E Kerrouchea, A. Mezouara, L. Boumedienea, A.V.D Bosscheb. Modeling and Lyapunov-Designed based on Adaptive Gain Sliding Mode Control for Wind Turbines. Journal of Power Technologies, Vol. 96, No. 2, 2016, pp. 124–136.

[16] M.A.A. Morsy, M. Said, A. Moteleb, H.T. Dorrah. Design and implementation of fuzzy sliding mode controller for switched reluctance motor. In: IEEE 2008 International Conference on Industrial Technology, 21-24 April 2008; Chengdu, China: IEEE. pp. 1367-1372.

[17] C. Lascu, F. Blaabjerg. Super-twisting sliding mode direct torque control of induction machine drives. In: IEEE 2014 *Energy Conversion Congress and Exposition*, 14-18 September 2014, Pittsburgh, PA: IEEE. pp. 5116-5122.

[18] S. Benelghali. On multiphysics modeling and control of marine current turbine systems. PHD, Bretagne Occidentale University, France, 2009.

[19] M. Das, C. Mahanta. Disturbance observer based optimal second order sliding mode controller for nonlinear systems with mismatched uncertainty. *IEEE First International Conference on Control, Measurement and Instrumentation (CMI)*, 8-10 January 2016, Kolkata, pp. 361-365.

[20] S.S Butt, R. Prabel and H. Aschemann. Second-Order Sliding Mode Control of an Innovative Engine Cooling System. Industrial Electronics Society, IECON 2015 - 41st Annual Conference of the IEEE. November 9-12, 2015, Yokohama, pp. 2479-2484.

[21] A. Levant, L. Alelishvili. Integral high-order sliding modes. IEEE T Automat Contr 2007; 52: 1278-1282.

[22] A. Levant. Higher-order sliding modes, differentiation and output feedback control. Int J Control 2003; 76: 924-941.

[23] F. Amrane, A. Chaiba, S. Mekhilef. High performances of Grid-connected DFIG based on Direct Power Control with Fixed Switching Frequency via MPPT Strategy using MRAC and Neuro-Fuzzy Control. Journal of Power Technologies 96 (1) (2016) 27–39.

[24] M.R. Baiju, K. Gopakumar, K.K. Mohapatra, V.T. Somasekhar and L. Umanand. Five-level inverter voltage-space phasor generation for an open-end winding induction motor drive. IEE P-Elect Pow Appl 2003; 150: 531-538.

[25] W.J. Wang, J.Y. Chen. Passivity-based sliding mode position control for induction motor drives. IEEE T Energy Conver 2005; 20: 316-321.

[26] J.J.E. Slotine. Sliding controller design for nonlinear systems. Int J Control 1984; 40: 421-434.

[27] B. Beltran, M.E.H. Benbouzid, -Ali T. Ahmed. High-order sliding mode control of a DFIG-based wind turbine for power maximization and grid fault tolerance. In: IEEE 2009 International Electric Machines and Drives Conference, May 2009; Miami, Florida, USA: IEEE. pp. 183-189.

[28] B. Beltran, M.H. Benbouzid, -Ali T. Ahmed. Second-order sliding mode control of a doubly fed induction generator driven wind turbine. IEEE T Energy Conver 2012; 27: 261-269.

[29] S. Benelghali, M.E.H. Benbouzid, J.F. Charpentier, T. Ahmed-Ali, I. Munteanu. Experimental validation of a marine current turbine simulator: Application to a PMSG-based system second-order sliding mode control. IEEE T Ind Electron 2011; 58: 118-126.

Ahmed Bourouina received his M.Sc. degree in Electrical Engineering from National Polytechnic School, Oran, Algeria, in 2012.Currently,he is a PhD student in the same school. His research activities consist of robust control strategies, power electronics, electrical machine drives and renewable energies.

Abdelkader Djahbar received his Ph.D. degree in electrical engineering and habilitation to lead researches from the Mohamed Boudiaf University of Science and Technology of Oran (USTO), Algeria, in 2008, 2012 respectively. In December 2002, he joined the electrical engineering department of the Hassiba Ben Bouali Univesity of Chlef, Algeria. Since July 2017, he has been a Professor in the same department.Since April 2014 he has been an associate researcher at the LMOPS laboratory of the Université de Lorraine and Centrale Supélec and and since 2013 a researcher at the GEER laboratory of UHBC. His scientific work is related to electrical machines and drives and power electronics. His present research interest is in multi machine drives, matrix converter and power quality.

Abdelkader Chaker received his Ph.D. degree in Engineering Systems from the University of Saint-Petersburg in 2002.Currently he is a Professor in the Department of Electrical Engineering at the ENP, in Oran Algeria. His research activities include control of large power systems, multimachine multiconverter systems and unified power-flow controllers. His teaching themes are neural process control and real-time simulation of power systems.

Zinelaabidine Boudjema is Teacher at the University of Chlef, Algeria. He received his M.Sc. degree in electrical engineering from ENP of Oran, Algeria in 2010 and his PhD degree, in Electrical Engineering from the University of Sidi-Belabbes, Algeria, in 2015. His research activities include the study and application of robust control in wind-solar power systems.